View metadata, citation and similar papers at core.ac.uk
brought to you by CORE
provided by Elsevier - Publisher Connector

Systematic Heterogeneity of Fractional Vesicle Pool Sizes and Release Rates of Hippocampal Synapses

Oliver Welzel,[†△] Andreas W. Henkel,[‡△] Armin M. Stroebel,[†] Jasmin Jung,[†] Carsten H. Tischbirek,[†] Katrin Ebert,[†] Johannes Kornhuber,[†] Silvio O. Rizzoli,[§] and Teja W. Groemer[†*]

[†]Department of Psychiatry and Psychotherapy, University of Erlangen-Nuremberg, Erlangen, Germany; [‡]Department of Physiology, Faculty of Medicine, Jabriya, Kuwait University, Safat, Kuwait; and [§]European Neuroscience Institute Göttingen, Deutsche Forschungsgemeinschaft Research Center for Molecular Physiology of the Brain/Excellence Cluster 171, Göttingen, Germany

ABSTRACT Hippocampal neurons in tissue culture develop functional synapses that exhibit considerable variation in synaptic vesicle content (20–350 vesicles). We examined absolute and fractional parameters of synaptic vesicle exocytosis of individual synapses. Their correlation to vesicle content was determined by activity-dependent discharge of FM-styryl dyes. At high frequency stimulation (30 Hz), synapses with large recycling pools released higher amounts of dye, but showed a lower fractional release compared to synapses that contained fewer vesicles. This effect gradually vanished at lower frequencies when stimulation was triggered at 20 Hz and 10 Hz, respectively. Live-cell antibody staining with anti-synaptotagmin-1-cypHer 5, and overexpression of synaptopHluorin as well as photoconversion of FM 1-43 followed by electron microscopy, consolidated the findings obtained with FM-styryl dyes. We found that the readily releasable pool grew with a power function with a coefficient of 2/3, possibly indicating a synaptic volume/surface dependency. This observation could be explained by assigning the rate-limiting factor for vesicle exocytosis at high frequency stimulation to the available active zone surface that is proportionally smaller in synapses with larger volumes.

INTRODUCTION

Synapses in a rat hippocampal tissue culture hold between 20 and 350 synaptic vesicles (1,2), which are able to release their content into the synaptic cleft upon fusion with the plasma membrane at the active zone. In static ultrastructural images, vesicles seem to form a homogeneous collective. However they are organized in highly dynamic intermixing functional groups, the vesicle pools (3). The readily releasable pool (RRP) of 5–10 vesicles is already docked to the active zone and primed for fusion. The RRP can be released immediately upon a rapid stimulation with 40 action potentials (4,5). During prolonged stimulation, the rate of vesicle release, and thus the probability for fusion, decreases as the readily releasable pool becomes exhausted. If the stimulus continues, vesicles from the recycling pool begin to be exocytosed. The recycling pool of synapses in rat hippocampal tissue cultures comprises ~130 vesicles (6) and can be depleted by 900–1200 action potentials (7–9). The reserve pool is believed to be hardly turned over by physiological activity (5).

To analyze the distinct vesicle pools, in addition to the patch-clamp technique (10–12) and electron microscopy (13–15), fluorescence microscopy has been employed for its inherent advantage of spatial and temporal resolution. Especially styryl dyes, introduced by Betz and Bewick (16), have been extensively used to determine functional features of presynaptic boutons. These dyes become fluorescent when integrated in the membrane. Using electrical stimulation, dye can be loaded into synaptic vesicles by compensatory endocytosis. If plasma membrane-inserted dye is subsequently removed by washing with dye-free medium, fluorescence is observed in puncta corresponding to synaptic terminals (14,17). Other optical methods to investigate synaptic vesicle recycling and vesicle pool characteristics include the overexpression of synaptopHluorin (spH), a pH-sensitive GFP variant coupled to the vesicular protein synaptobrevin-2 (18,19) and the uptake of a CypHer 5 labeled antibody against synaptotagmin1 (αSyt1-cypHer 5) (20,21), which we have also previously shown to be suitable for kinetic measurements of vesicular release (2).

Using these techniques, it was shown that vesicle numbers, pool sizes, and release probabilities typically show a distribution skewed positively to the right (4,6,8,22,23), and vary considerably and systematically between individual synapses (22–24). These parameters determine the individual synapse's efficacy of signal transmission and are thought to be a crucial factor for the regulation of information processing in neural networks (4,25).

Ultrastructural studies revealed that the number of synaptic vesicles increases with the bouton volume (4,26). Thereby the volume of synapses can easily vary by a factor of 20 (26). The area of the active zone also correlates positively with the bouton volume, and thus the number of vesicles (26). The variation of the active zone size is smaller than the variation of the synaptic volume (26), while the

Submitted July 26, 2010, and accepted for publication December 14, 2010.

△Oliver Welzel and Andreas W. Henkel contributed equally to this work.

*Correspondence: teja.groemer@uk-erlangen.de

This is an Open Access article distributed under the terms of the Creative Commons-Attribution Noncommercial License (http://creativecommons.org/licenses/by-nc/2.0/), which permits unrestricted noncommercial use, distribution, and reproduction in any medium, provided the original work is properly cited.

Editor: Paul W. Wiseman.

© 2011 by the Biophysical Society

0006-3495/11/02/0593/9 $2.00

doi: 10.1016/j.bpj.2010.12.3706

density of docked vesicles is preserved at the active zone (1). A direct influence of these morphological features on the distinct vesicle pools, synaptic vesicle release velocities, and rates, however, has remained elusive.

In this study, we analyzed the functional and structural parameters of individual synapses and investigated their individual pool sizes by vesicle quantum fluorescence determination complemented with novel pool size determination assays based on spH or αSyt1-cypHer 5 as well as photoconversion of FM 1–43 followed by electron microscopy. We are able to report an inverse correlation between recycling pool and fractional vesicular release. We show that synapses with large recycling pool sizes exhibit a smaller fraction of RRP vesicles when compared with synapses with small recycling pool sizes. We furthermore provide evidence for a power law relationship between these parameters that could point to a simple geometric constraint, namely the ratio between the surface area of the active zone and the volume of the presynaptic bouton.

MATERIALS AND METHODS

Cell culture and transfection

Hippocampal neuronal cultures were prepared from one-to-three-days-old Wistar rats (Charles River, Wilmington, MA) as described (2). Newborn rats were killed by decapitation in accordance with the guidelines of the State of Bavaria. Hippocampi were removed from the brain and transferred into ice cold Hank's salt solution, and the dentate gyrus was cut away. After digestion with trypsin (5 mg mL^{-1}) cells were triturated mechanically and plated in MEM medium, supplemented with 10% fetal calf serum and 2% B27 Supplement (all from Invitrogen, Taufkirchen, Germany). If required, neurons were transfected with synaptopHluorin under control of a synapsin promoter (27) on DIV3 with a modified calcium phosphate method as described (2,28). Experiments were performed between 18 and 22 days in vitro.

Imaging

Experiments were conducted at room temperature on a TI-Eclipse inverted microscope (Nikon, Melville, NY) equipped with a 60×, 1.2 NA water immersion objective and Perfect Focus System (Nikon). Fluorescent dyes were excited by an Intensilight C-HGFI (Nikon) through excitation filters centered at 482 nm, 561 nm, and 628 nm using dichroic long-pass mirrors (cutoff wavelength 500 nm, 570 nm, and 660 nm), respectively. The emitted light passed through emission band-pass filters ranging from 500 nm to 550 nm, 570 nm to 640 nm, and 660 nm to 730 nm, respectively (Semrock, Rochester, NY) and was projected onto a cooled electron-microscopy (EM) charge-coupled device camera (iXon^{EM} DU-885 and iXon^{EM} DU-897; Andor Technology, Belfast, Ireland).

Coverslips were placed into a perfusion chamber (volume = 500 μL) containing extracellular medium containing 144 mM NaCl, 2.5 mM KCl, 2.5 mM $CaCl_2$, 2.5 mM $MgCl_2$, 10 mM Glucose, and 10 mM HEPES, pH 7.5. Synaptic boutons were stimulated by electric field stimulation (platinum electrodes, 10-mm spacing, 1-ms pulses of 50 mA and alternating polarity); 10 μM 6-cyano-7-nitroquinoxaline-2,3-dione (Tocris Bioscience, Bristol, Avon, United Kingdom) and 50 μM D-amino-5-phosphonovaleric acid (Tocris Bioscience) were added to prevent recurrent activity.

Recycled synaptic vesicles were labeled with FM 1-43, FM 4-64, and FM 5-95 (Invitrogen, Karlsruhe, Germany). To stain the total recycling pool, nerve terminals were loaded with 1200 pulses at 40 Hz (7–9) using 2.5 μM FM 1-43, 2.5 μM FM 4-64, and 15 μM FM 5-95, respectively. Dyes were allowed to remain on the cells for 60 s after stimulation was finished to permit complete endocytosis, and were subsequently removed by a 7-min washout. The loaded boutons were then stimulated with 600 pulses at 30 Hz, 20 Hz, or 10 Hz, respectively, to evoke exocytosis. To obtain a measure for the total amount of loaded vesicles we completely destained boutons using a twofold stimulation with 900 pulses at 30 Hz (29). Images were recorded with 200-ms exposure time at 0.5 Hz frame rate and 500-ms exposure time at 2 Hz frame rate for the stimulation with 600 pulses, respectively.

The frame rate was 0.25 Hz for double total destain stimulation regime with 900 pulses. For the measurement of quantum intensities, we performed subtotal staining experiments (20 pulses at 0.5 Hz) as described in Murthy et al. (22). Loaded boutons were completely destained with two consecutive stimulations of 300 pulses and 600 pulses at 5 Hz. Images were recorded with 500-ms exposure time at 0.05 Hz frame rate. To measure the readily releasable pool, boutons were loaded with 1200 pulses at 40 Hz using 5 μM FM 4-64 and afterwards stimulated with 40 pulses at 20 Hz (4,5). Boutons were completely destained with two consecutive stimulations of 900 pulses at 30 Hz. Images were recorded with 200-ms exposure time at 1 Hz frame rate.

For the anti-synaptotagmin-1-cypHer 5 experiments, cultured dispersed hippocampal neurons were incubated for 2 h with 0.6 μg of CypHer 5E labeled anti-synaptotagmin1 antibody (αSyt1-cypHer 5) (Synaptic Systems, Göttingen, Germany) in extracellular medium to stain synaptic boutons. Cells were electrically stimulated with 40 pulses at 20 Hz followed by 1200 pulses at 40 Hz in the presence of the v-ATPase blocker folimycin (80 nM). Images were recorded with 2000-ms exposure time at a frame rate of 0.2 Hz.

In the synaptopHluorin experiments, boutons were stimulated with 600 pulses at 30 Hz or 40 pulses at 20 Hz followed by 1200 pulses at 40 Hz in the presence of 80 nM folimycin. Images were recorded with 200-ms and 300-ms exposure time, respectively, at a frame rate of 1 Hz. For all experiments, resulting image stacks were converted into tagged image file format.

Electron microscopy

For electron microscopy, cell cultures were grown on Thermanox coverslips (Plano, Marburg, Germany), stimulated with 40 pulses at 20 Hz in the presence of 10 μM FM 1-43 (Biotium, Hayward, CA), allowed to recover for 30 s, and fixed, photoconverted, and processed for electron microscopy as described (15,30).

Data analysis

See Materials and Methods in the Supporting Material.

Computer simulations

See Materials and Methods in the Supporting Material.

RESULTS

Synapses with large recycling pools exhibit higher release time constants

The recycling pool of synapses was stained with FM 1-43 as described (7). Synaptic terminals showed a typical punctuated fluorescence pattern (16,17) (Fig. 1 *A*, *left*). To ensure that FM 1-43 labels neuronal synapses, we additionally labeled functional terminals with a monoclonal antibody directed against the intravesicular domain of synaptotagmin-1. This monoclonal antibody was coupled to the pH-sensitive Cy5 dye variant CypHer 5 (αSyt1-CypHer 5). Colocalization

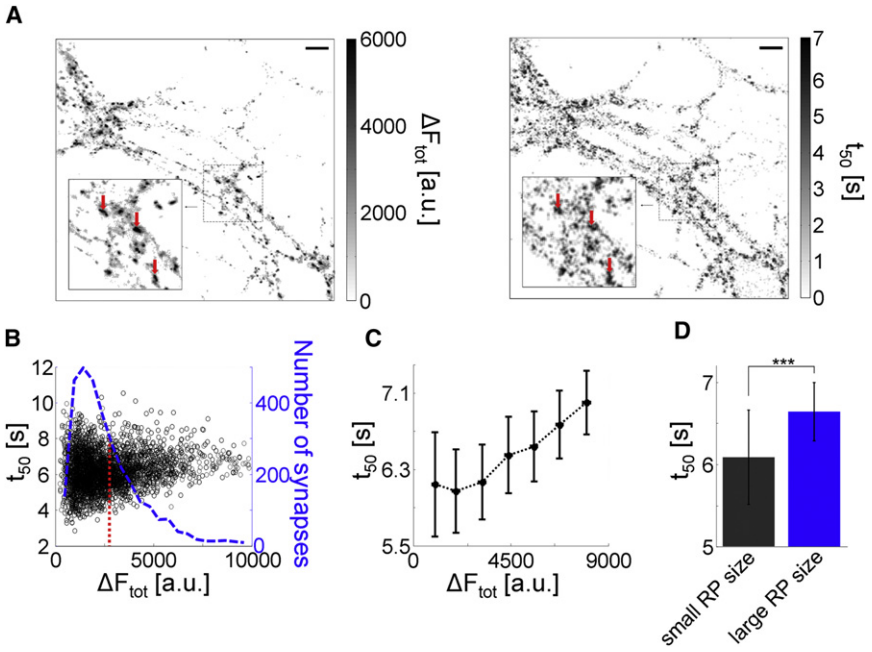

FIGURE 1 Spatial distribution and relation between recycling pool size ΔF_{tot} and electrically evoked FM1-43 release half-decay time constant t_{50}. (*A*) (*Left*) Difference-image of FM 1-43 labeled neurons in a typical experiment. Presynaptic terminals were maximally loaded with 1200 pulses at 40 Hz. A test pulse of 600 pulses at 30 Hz was applied after washing and synapses were completely destained by two subsequent stimulation cycles with 900 pulses at 30 Hz. (*Right*) The fluorescence half-decay time constants from the left image during stimulation were calculated to generate a time constant image. Synapses with large recycling pool size colocalize with areas of high t_{50} values (*red arrows*; scale bars 11 μm). (*B*) Synapse fluorescence intensity histogram (*bold dotted blue line*) and correlation between recycling pool size ΔF_{tot} and half-decay time constants t_{50} (Spearman's $\rho = 0.23 \pm 0.07$, $p < 0.05$), derived from individual synapses (*black circles*, 3149 synapses, five experiments). The mean value of ΔF_{tot} (2620 a.u.) is indicated by the red dotted line. (*C*) Synapses were grouped in bins and averaged. t_{50} values were normal distributed affirmed by one-sample Kolmogorov-Smirnov test in each group and significant different (one-way ANOVA: $F_{6,31} = 17.23$; $p < 0.001$). The half-decay time t_{50} increases with increasing ΔF_{tot} with a strong effect size (Cohen's $d = 1.10 \pm 0.18$). (*D*) Synapses with large recycling pool (RP) sizes released their dye content relatively slower than synapses with small recycling pool sizes (two-sample *t*-test, *** $p < 0.001$; 315 synapses). All error bars indicate standard error of the mean.

analysis reveals that FM 1-43 labels neuronal synapses (see Fig. S1 in the Supporting Material; Mander's overlap (31) = 0.94 ± 0.007).

It has been shown that the intensity of FM-staining corresponds to the number of stained vesicles in individual synapses (32,33) so that the fluorescence amplitude reflects the size of the recycling pool. The distribution of recycling pool sizes was skewed to the right and therefore synapses with large recycling pools were rare (Fig. 1 *B*). This distribution was consistently observed in all neuronal cultures (Fig. 1 *B*). After recycling pool labeling, fluorescence was released by electrical stimulation and half-decay time constants t_{50} were recorded for all synapses. We found that synapses with high recycling pool sizes had higher half-decay time constants, indicated by a Spearman's coefficient of $\rho = 0.23 \pm 0.07$, $p < 0.05$ with a large effect size (34) of Cohen's d of 1.10 ± 0.18 (Fig. 1 *A*, *right*).

Afterwards, synapses were grouped in equally spaced recycling pool size bins. We found that t_{50} values continuously increased with recycling pool size (Fig. 1 *C*). The difference between the means of the smallest and largest recycling pool bins was 0.86 s (14% increase). Half-decay time constants were normally distributed in each bin, as confirmed by one-sample Kolmogorov-Smirnov test and significantly different (one-way ANOVA: $F_{6,31} = 17.23$, $p < 0.001$). Thus synapses with large recycling pool sizes released their dye content relatively more slowly than synapses with small recycling pool sizes (two-sample *t*-test: $p < 0.001$) (Fig. 1 *D*). Interestingly, reduction of stimulation frequency to 20 Hz reduced this effect, largely as indicated by a weaker effect size (Cohen's $d = 0.59 \pm 0.13$). Additionally, the positive correlation between fluorescence and half-decay time t_{50} was no more statistically significant (see Fig. S3; Spearman's $\rho = 0.09 \pm 0.03$, $p > 0.15$; 3092 synapses, five experiments). Further frequency reduction to 10 Hz confirmed this trend (see Fig. S3; Cohen's $d = 0.45 \pm 0.15$; Spearman's $\rho = 0.01 \pm 0.04$, $p > 0.3$; 2010 synapses, three experiments).

The effect, however, prevailed, when other FM dyes like FM 4-64 (Cohen's $d = 0.88 \pm 0.33$; Spearman's $\rho = 0.17 \pm 0.05$, $p < 0.05$; 1630 synapses, three experiments) and FM 5-95 (Cohen's $d = 0.94 \pm 0.36$; Spearman's $\rho = 0.15 \pm 0.05$, $p < 0.05$; 1571 synapses, three experiments) were used. In an overexpression approach, we transfected hippocampal neurons with spH, which can also be used to define functional synaptic boutons (18) and marks the amount of exocytosed vesicles (19). Presynaptic terminals were stimulated in the presence of folimycin to block reacidification and thus have a measure of net exocytosis. Again, synapses with high recycling pool sizes had higher fluorescence increase time constants (see Fig. S2; Spearman's $\rho = 0.43 \pm 0.10$, $p < 0.05$; Cohen's $d = 0.81 \pm 0.37$).

Disuse hypersensitivity leads to higher release time constants

We then tested whether increasing the average recycling pool size has an effect on half-decay time constants.

Because it was shown that prolonged synaptic inactivity increased the size of synapses (4,35), we employed this disuse hypersensitivity model and inhibited recurrent autostimulation within the preparations by incubation with 500 nM TTX for three days. Compared to control preparations, the recycling pool size increased by 10.5% and corresponding t_{50} increased by 20% (6.82 s ± 0.17 s, controls: 5.68 s ± 0.18 s; two-sample t-test: $p < 0.001$; Fig. 2). This observation confirms that increased half-decay time t_{50} is directly linked to larger synapses.

Measurement of time constants was not affected by stimulation and appraisal artifacts

It was tested whether the intense stimulation used for loading the recycling pool in FM dye experiments itself affects the synaptic parameters like half-decay time t_{50}, e.g., by inducing plasticity. Therefore, hippocampal neurons were transfected with synaptopHluorin and boutons were first stimulated with 600 pulses at 30 Hz, which was used as reference stimulus. Cells were then stimulated with 1200 pulses at 40 Hz, as used in loading protocol of FM dye experiments. After adherence of 7-min waiting time, which corresponds to the time used for washing in FM dye experiments, cells were stimulated again with 600 pulses at 30 Hz. Comparison of fluorescence changes ΔF and the exocytosis and endocytosis kinetics revealed no significant or relevant differences between the reference stimulus and the second 600 pulses stimulus (Fig. S4). We conclude that the intense loading stimulus had no effect on the investigated synaptic parameters during the experimental time used here.

We next tested whether the chosen region-of-interest (ROI) size may be responsible for an artificial correlation between the pool size and t_{50}. Using the assumption that synapses with large recycling pool release more vesicles, it might be possible that an oversized ROI could result in a slower apparent vesicle release, if the released fluorescence was diffusing more slowly from the ROI. Therefore we reduced the radius of the ROI size to one or two pixels, respectively, and calculated the correlation together with the effect size again (one pixel: Cohen's $d = 0.89 \pm 0.18$; Spearman's $\rho = 0.21 \pm 0.06$, $p < 0.05$; two pixels: Cohen's $d = 1.10 \pm 0.16$; Spearman's $\rho = 0.21 \pm 0.07$, $p < 0.05$). The results clearly indicated that the effect was independent of the ROI size.

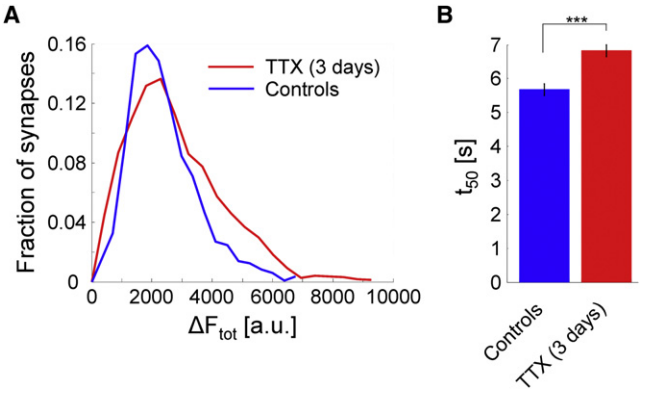

FIGURE 2 Disuse hypersensitivity leads to higher release time constants. (*A*) Histograms for preparations incubated with 500 nM TTX for three days (1526 synapses, three experiments) and control preparations (1748 synapses, three experiments), respectively. Disuse hypersensitivity increased recycling pool size by 10.5%. (*B*) Corresponding t_{50} increased by 20% (two-sample t-test, $p < 0.001$). Error bars indicate standard deviation.

We then tested whether synapses with smaller recycling pool sizes have a larger half-decay time constant variation due to their low fluorescence signal/noise ratio (SNR). This potential error is expected to decrease with increasing SNR, leading to an increasingly accurate time-constant at lower noise levels. To address this and the following appraisal problems, we generated images with simulated scattered virtual synapses, represented by two-dimensional rotation-symmetric Gaussian profiles with the standard deviation σ, sampling rates, and fluorescence half-decay time constants, matching the experimental data. Half-decay time constants were measured in simulated and in real datasets (Fig. S5 *A*).

For increasing ΔF_{tot} and thus increasing SNR, t_{50} converged toward the preset value of $t_{50} = 6.6$ s in simulated datasets. The data from Fig. S1 *A* was binned and displayed in Fig. S5 *B*. This panel shows that the error rate increased and t_{50} became slightly overestimated for lower SNR ($\Delta F_{tot} < 1500$ arbitrary units (a.u.)). Experimentally obtained data, however, did not converge to a fixed value but showed a significant positive correlation between ΔF_{tot} and t_{50}, which is contrary to the results obtained from the computer generated images and therefore cannot be attributed to a low SNR.

We further measured the effect of increasing noise on our peak detection and time constant measurements. The mean spot detection probability was 90.31% ± 1.66% for all $SNR > 1$. The absolute error of t_{50} determination approximated zero for increasing SNR with a mean coefficient of variation of 0.02 and a maximal absolute error of ~0.1 s at SNR 1. The spot detection and the determination of t_{50} are thus almost completely independent of the SNR in our analyzed images.

We also tested whether the accuracy of time constant determination depended on the magnitude of the time constant itself and on the length of the time-series. In simulated datasets, the absolute error converged toward zero with increasing t_{50}. Here a mean coefficient of variation of 0.0039 and a relatively small maximal error of ~0.15 s at the lowest t_{50} was observed. This shows that the time constant magnitude does not impede t_{50} determination accuracy. Taken together, these simulations provide evidence that the maximal error induced by our detection and determination method was far too small to explain the measured difference of ~1 s in t_{50} between smallest and largest synapse groups.

We next tested whether the exclusion criterion, in the form of the coefficient of determination for the least-squared error fit used for the time constant determination, could bias against synapses that tend to have high half-decay time constants (see Materials and Methods). Therefore, we removed the exclusion criterion and calculated the correlation together with the effect size again (Cohen's $d = 0.99 \pm 0.25$; Spearman's $\rho = 0.24 \pm 0.09$, $p < 0.05$). The results clearly indicated that the effect is not influenced by the exclusion criterion in the form of the coefficient of determination.

Another potential kinetic influence on time constants is exerted by fluorescence bleaching. Some studies, e.g., Chen et al. (36), used fluorescence profile correction algorithms to avoid this problem. To test the effect of bleaching in our datasets, we measured the fluorescence profile slopes before, during, and after the electrical stimulation period. The means and standard deviations of the slopes were: -0.0016 ± 0.0024 (before stimulation), -0.0230 ± 0.0069 (during stimulation), and -0.0011 ± 0.000549 (after stimulation) (Fig. S6). When estimated from the period before stimulation, bleaching would have been limited to <7% of the fluorescence loss during the stimulation period, and therefore we did not correct for bleaching. Moreover, there was no overlap between the slopes of stimulation and resting periods. Taken together, all results show that determination of time constants was not affected by appraisal artifacts.

Different ratios of readily releasable pool to recycling pool in individual synapses

To compare the absolute and fractional number of released vesicles during high frequency stimulation between synapses with small and large recycling pool sizes, we first conducted subtotal staining experiments, using 20 pulses at 0.5 Hz to determine the fluorescence of a single vesicle as described (22) (Fig. S7). To analyze the quantization, we applied multi-Gaussian fits to the fluorescence intensity histogram of each experiment with the prerequisite of constant half-widths for all Gaussians, allowing for varying amplitudes and means. We found a clear quantal distribution with almost constant center-to-center differences of 20.02 ± 1.91 arbitrary units, which corresponded to the fluorescence of a single vesicle.

Fluorescence profiles were binned according to recycling pool size and averaged. As expected, the amount of absolute released vesicles was higher for synapses with large recycling pool size as indicated in Fig. 3 *A*. On the contrary, their relative number is smaller compared to synapses with small recycling pool size (Fig. 3 *B*). Thus, absolute and relative counterparts exhibited an inverse behavior (Fig. 3). In accordance with t_{50}, this shows that synapses with large recycling pool sizes released fewer vesicles relative to their recycling pool size.

Next, we wanted to know the maximal number of mobilized vesicles at individual active zones as these could be a limiting factor for maximal vesicle release during high frequency stimulation. For that purpose, we measured the RRP, which corresponds to directly docked vesicles at the active zone (12). Again, the recycling pool of synapses was stained with FM 4-64, as described in Ryan and Smith (7). The quantal analysis for FM 4-64 revealed a single vesicle fluorescence of 11.55 ± 1.62 arbitrary units (1093 synapses, three experiments).

The size of the RRP was measured by using a stimulus of 40 pulses at 20 Hz (4,5) and consists of 4.12 ± 2.65 vesicles (2836 synapses, four experiments) in accordance with previous studies (5,37).

As a measure for the total recycling pool (RP), we completely destained boutons using a twofold stimulation with 900 pulses at 30 Hz (29) (see Fig. 4, *A* and *B*). Next, we built the RRP/RP ratio for synapses with large and small recycling pool sizes, respectively (Fig. 4 *B*; large RP: 0.07 ± 0.007; small RP: 0.13 ± 0.02; two-sample *t*-test: $p < 0.001$; 294 synapses, four experiments). Thus, synapses with large recycling pools had a smaller RRP fraction compared to synapses with small recycling pools. To exclude that the difference in the RRP/RP ratio is a phenomenon of styryl-dye labeling, we tested sets of experiments in which we had used a synaptopHluorin overexpression (spH) approach as well as an antibody-based functional labeling system (αSyt1-CypHer 5) for their compatibility with the results from FM-dye labeling.

Using αSyt1-CypHer 5 enabled us to label functional terminals selectively, because CypHer 5 fluoresces in the

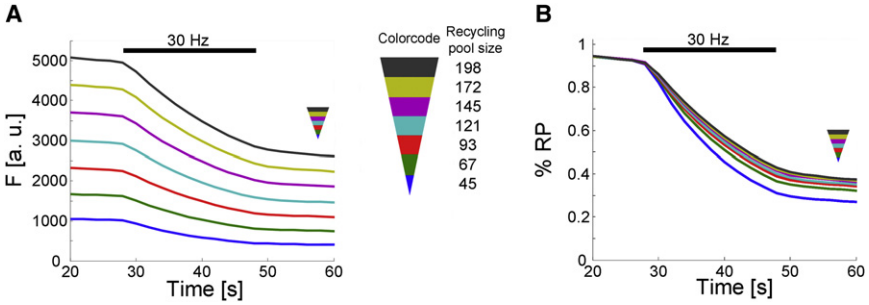

FIGURE 3 Absolute and relative fluorescence release in recycling pool size groups (8481 synapses, nine experiments). Fluorescence profiles were binned according to recycling pool size and were averaged. A triangular legend symbol indicates the smallest (*tip* of the *triangle*) and largest (*base* of the *triangle*) recycling pool size. Fluorescence profiles of the different recycling pool size bins in absolute (*A*) and relative values (*B*).

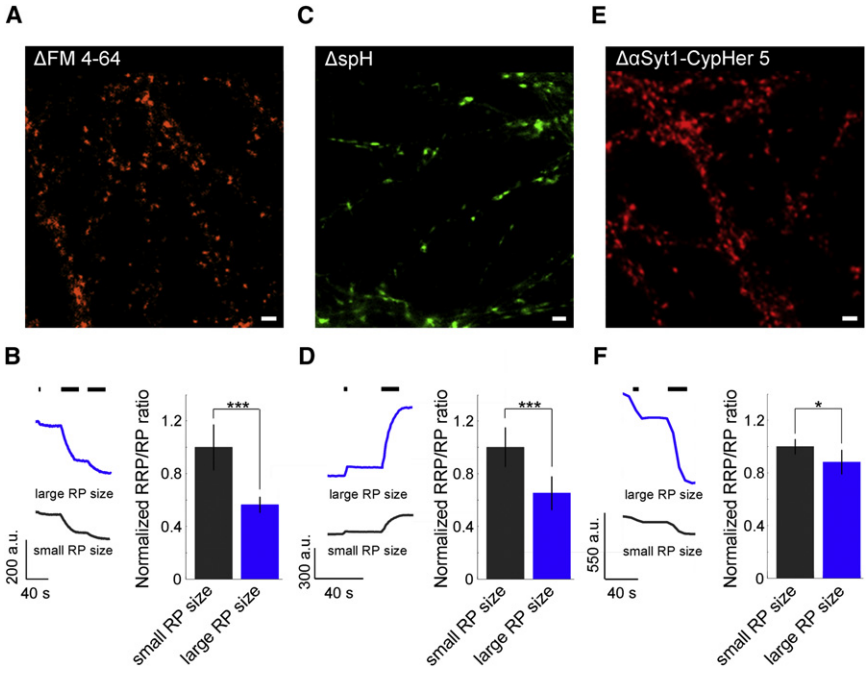

FIGURE 4 Ratio of readily releasable pool (RRP) to recycling pool (RP) for different pool sizes in three different functional fluorescence labeling approaches. (*A*, *C*, and *E*) Representative fluorescence difference images of (*A*) FM 4-64, (*C*) synaptopHluorin, and (*E*) αSyt1-CypHer 5 before and after electrical stimulation (Scale bars, 3 μm). Presynaptic terminals were stimulated with 40 pulses at 20 Hz as a measure for the RRP followed by a twofold stimulation with 900 pulses or a single stimulation with 1200 pulses as a measure for the RP. (*B*, *D*, and *F*) Synapses were grouped according to their recycling pool size (see Materials and Methods). Fluorescence time courses and normalized ratio of RRP to RP of synapses with small and large RP sizes in FM 4-64 (*B*) (294 synapses, four experiments), synaptopHluorin (*D*) (494 synapses, six experiments), and αSyt1-CypHer 5 (*F*) (639 synapses, five experiments) labeling experiments. In synaptopHluorin and αSyt1-CypHer experiments, terminals were stimulated in the presence of folimycin to block reacidification. (Scale bars, 3 μm; two-sample *t*-test, * $p < 0.05$, *** $p < 0.001$). Error bars indicate standard deviation.

acidic milieu of synaptic vesicles (pH 5.5) but not if exposed to extracellular pH (pH 7.4). In addition to the selective labeling of functional terminals by their antibody uptake, it enables visualization of synaptic exo- and endocytosis cycles according to the stimulation-dependent change in fluorescence. In both approaches, presynaptic terminals were stimulated in the presence of v-ATPase blocker folimycin to permanently block reacidification of recycling vesicles to get a measure of pool sizes. The different functional fluorescence labeling approaches affirmed the results obtained with FM 4-64 (see Fig. 4, *C–F*). The RRP/RP ratio in αSyt1-CypHer 5 experiments (Fig. 4 *F*) exhibited a smaller difference compared to FM 4-64 labeling and synaptopHluorin experiments (Fig. 4, *B* and *D*). This is most likely because incubation with an antibody for 2 h does not stain the whole recycling pool.

Given these findings, we sought to qualitatively confirm our results resorting to FM 1-43 labeling followed by photoconversion (photooxidation) of the dye (14,15,30), which could be visualized in electron microscopy afterwards (Fig. 5 *A*). The number of recycled synaptic vesicles after 40 pulses at 20 Hz was counted for each section of a presynaptic terminal and the percent of labeled vesicles per section was calculated. In accordance with results obtained from fluorescence microscopy, large synapse sections with a high number of vesicles had a lower percentage of labeled vesicles per section (Fig. 5, *B* and *C*; two-sample *t*-test: $p < 0.001$; 133 synapses).

One possible source of error in using thin sections, however, could be that a synapse with large recycling pool is cut in a way, e.g., at a border, that it appears as a synapse with a small section. Using this technique, however, a small synapse cannot be cut in a manner that yields a large section. Given that synapses with small recycling pool sizes outnumber large synapses, the contribution of small border-sections of large terminals to the small terminal sections should be minor. Moreover, the error that could be introduced by peripheral cross sections of large synapses (which would be falsely classified as a small synapse) would decrease the apparent RRP fraction of the synaptic vesicle pool at small cross sections, which is not what we have found here.

The kinetics of exocytosis is limited by the surface/volume relationship

What mechanism determines the positive correlation between t_{50} and recycling pool size at high (30 Hz) stimulation frequency?

Half-decay times t_{50} should be identical in synapses with large and small recycling pool sizes if a constant proportion of vesicles was released at all synapses. By knowing the number of maximal mobilized vesicles, which correspond to the RRP, we calculated the relation between RRP and the RP. This relation is likely to be determined by the geometry of the synapse, because synaptic vesicles fuse within a defined surface area of the active zone during exocytosis.

If the number of mobilized vesicles and RP were connected in a surface/volume relationship, this relation should follow a power function, $m_{power} \cdot x^{2/3}$, where m is a scaling factor and the exponent 2/3 corresponds to active zone area/synaptic volume, because surfaces grow with an exponent of 2, and volumes with an exponent of 3. Fig. 6 shows that the

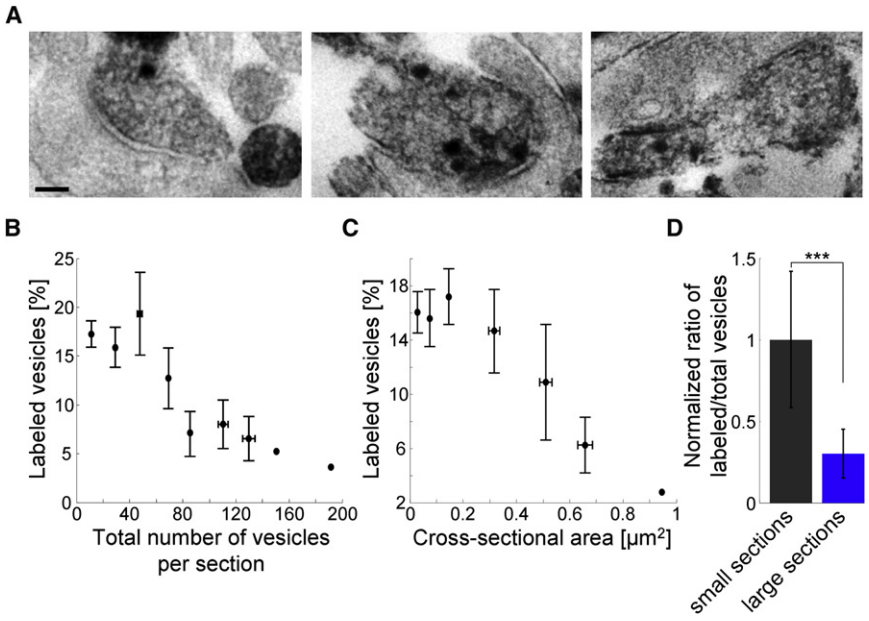

FIGURE 5 Electron microscopy affirmed the results obtained with fluorescence microscopy. (*A*) Recycled synaptic vesicles after 40 pulses at 20 Hz investigated by FM 1-43 uptake followed by photoconversion and electron microscopy. Note the dark (labeled) vesicles (Scale bar, 100 nm). (*B* and *C*) With increasing number of vesicles per cross section or cross-sectional area, the percentage of labeled vesicles decreases (133 synapses). (*D*) Normalized ratio of labeled vesicles to total vesicles of small and large cross-sections of terminals obtained from EM experiments (two-sample *t*-test, *** $p < 0.001$; 13 synapses). All error bars indicate standard deviation.

relation is well determined by a 2/3-exponent power function. Table S1 shows that a power function fit to the data was clearly better ($R^2 = 0.99$), compared to a linear fit ($R^2 = 0.80$). Additionally, the Schwarz-Bayes criterion (SBC) (38) favored the power function ($SBC = 29.86$) instead of the linear model ($SBC = 30.20$). The data from different functional fluorescence labeling approaches (spH and αSyt1-CypHer 5) confirmed these results (Fig. S8).

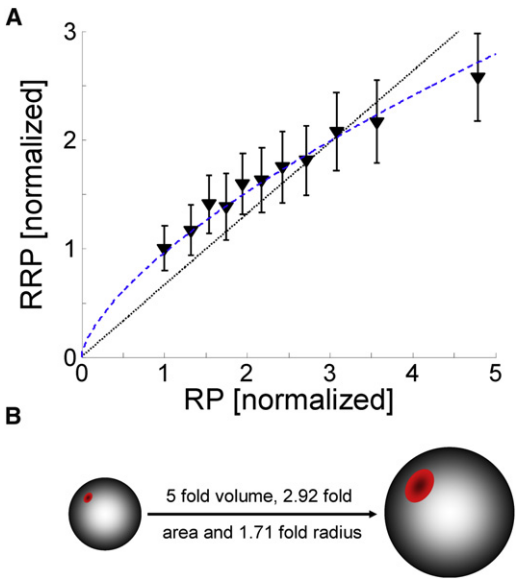

FIGURE 6 The relation between readily releasable pool (RRP) and recycling pool (RP) size obtained from FM 4-64 experiments fits to a volume to surface dependency, described by a power function: $m_{power} \cdot x^{2/3}$. (*A*) The RRP increases nonlinearly with the RP. A linear fit (*dashed black line*, $m_{linear} = 0.66$ (0.58, 0.73)) and a power function (*dashed blue line*, $m_{power} = 0.95$ (0.93, 0.98)) are shown. Error bars indicate standard error of the mean. (*B*) Surface volume relation visualized for spherical shape with an exemplary area.

DISCUSSION

Distribution and release parameters as well as release probabilities of individual synapses are in the focus of current research. Styryl dyes allowed us to study a variety of synaptic parameters such as spontaneous synaptic activity (39), the time-course of endocytosis (17), the release kinetics of individual synapses (22,23), analysis of different synaptic vesicle pools (10,29,40), and single synaptic vesicle exocytosis (32,33,36,41). In contrast to ultrastructural studies, fluorescence microscopy imaging allows the analysis of 10–100 times more synapses in a single experiment.

In this study, we addressed the issue of how the kinetics of synaptic vesicle exocytosis is connected to the synaptic vesicle pool composition. Using single vesicle fluorescence determination and recycling pool labeling, we were able to measure absolute and relative vesicle numbers. Here automated full population analysis provided the advantage of high numbers of synapses being investigated, a prerequisite for the measurement of relatively rare synapses with large recycling pool sizes and comparisons of time-constants. We showed that half-decay time constants of individual synapses were positively correlated with their recycling pool sizes. This effect was seen best at high frequencies (Fig. S3).

Fluorescence half-decay time constants t_{50} during stimulation have been extensively used to measure and compare FM dye release from synaptic vesicles. However, half-decay time determinations are prone to a variety of systematic

errors due to calculation artifacts. This is important, because the fluorescence brightness of synapses can vary in the order of two magnitudes and therefore shows a high range of the SNR variability. It was therefore necessary to provide controls to ensure that detection, determination, and quantification artifacts had no significant effect on accurate determination of time constants in our imaging setup and analysis system. Among other factors, different stimulation protocols, ROI sizes, noise, photobleaching, and the magnitude of the time constant itself were tested and found not to influence our results significantly.

Differences in half-decay time constants under specified experimental conditions were highly statistically significant, because we analyzed large numbers of synapses. We thus felt that the biological relevance of the finding was not best represented by the statistical significance level and therefore calculated the effect strength (34), which provides a sample size-independent estimation parameter. As measured by its strength, the effect was very strong and robust.

What mechanism underlies the positive correlation between t_{50} and recycling pool size?

Half-decay time constants are relative measures of vesicular release. This is underpinned by the fact that while a synapse with large recycling pool size releases more vesicles in absolute terms, its fractional release is smaller when compared to synapses with small recycling pool sizes (Fig. 3).

Different vesicle pools were categorized depending on their release kinetics (42). A difference in time constants of vesicular release therefore could originate from a difference in vesicle pool composition, i.e., the relative contribution of the readily releasable pool (RRP) of vesicles to the recycling pool (RP). We thus measured the readily releasable pool and the recycling pool of individual terminals in a variety of fluorescence assays as well as photoconversion of FM 1-43 followed by electron microscopy. We found that the RRP fraction is significantly smaller in terminals with large recycling pool sizes when compared to small recycling pool size terminals. This finding was consistent in all assays. Vesicle pool fractions therefore are heterogeneously distributed in hippocampal neurons.

What is the reason for the differences in the RRP/RP ratios observed?

Previous findings from ultrastructural studies indicate that the number of vesicles is directly proportional to the volume of the synapse (4,26). Moreover, synapses of different recycling pool sizes and thus volumes are identical in vesicle density (26) which is therefore independent of the synapses volume or vesicle number. The release probability, which increases with the size of the recycling pool (6,22), reflects the number of vesicles involved in repetitive exo-endocytosis cycles at the active zone (1), while directly docked vesicles comprise the RRP (12) and the density of vesicles per active zone area remains constant between synapses with different active zone sizes (1). Thus the RRP, directly measured in our experiments, can be assumed to reflect the area of the active zone, while the recycling pool corresponds to the synaptic volume. We have shown that synapses with large recycling pool sizes have higher half-decay time constants than synapses that contain fewer vesicles.

Given the above-presented structural considerations, this could originate from that the maximal release capacity of the active zone is reached earlier in synapses with small recycling pool sizes. If this was the case, the number of mobilized vesicles and the recycling pool size should be connected in a surface-to-volume relationship, their relation following a power function, $m_{power} \cdot x^{2/3}$, where m is a scaling factor and the exponent 2/3 corresponds to active zone area/synaptic volume, because surfaces grow with an exponent of 2, and volumes with an exponent of 3.

When correlating the recycling pool size with the readily releasable pool size, we found a nonlinear relation that is well fitted by that power function (Fig. 6). This is compatible with synapses with large recycling pool sizes holding a higher total vesicle number per active zone area, and thus containing relatively larger stores of vesicles. The growth of the active zone surface area might therefore be the limiting factor for increasing neurotransmitter release. This is underpinned by the finding that differences in release rate time constants are best seen at higher frequencies. However, because the vesicle count grows with the volume, far more stand-by vesicles are lined up after a released vesicle, if the recycling pool is large.

Under sustained stimulation conditions and thus constantly elevated intracellular calcium (43), transmission in synapses with large recycling pool sizes is not only greater in amplitude but also of higher relative stability. This is an important favorable feature of synapses with large recycling pool sizes concerning their contribution to transmission. With more vesicles released by synapses with large recycling pool sizes upon an action potential, high time constants correlate with higher release probabilities. Consequently, the dye released from synapses with fewer vesicles becomes faster depleted than in synapses with large recycling pool sizes, pointing to a higher sustenance of neurotransmitter release in terminals with high recycling pool sizes. Our results suggest that synaptic size and vesicle content determine sustenance, release probability, and release velocity of neurotransmitters, and this heterogeneous size distribution contributes to functional brain plasticity.

SUPPORTING MATERIAL

Eight figures and one table are available at http://www.biophysj.org/biophysj/supplemental/S0006-3495(10)05224-0.

This work was supported by the Erlanger Leistungsbezogene Anschubfinanzierung und Nachwuchsförderung ELAN grant No. PS-08-09-22-2 and by the Interdisciplinary Center of Clinical Research in Erlangen (Project No. J5) (both to T.W.G.).

REFERENCES

1. Schikorski, T., and C. F. Stevens. 1997. Quantitative ultrastructural analysis of hippocampal excitatory synapses. *J. Neurosci.* 17:5858–5867.
2. Welzel, O., C. H. Tischbirek, …, T. W. Groemer. 2010. Synapse clusters are preferentially formed by synapses with large recycling pool sizes. *PLoS ONE.* 5:e13514.
3. Rizzoli, S. O., and W. J. Betz. 2005. Synaptic vesicle pools. *Nat. Rev. Neurosci.* 6:57–69.
4. Murthy, V. N., T. Schikorski, …, Y. Zhu. 2001. Inactivity produces increases in neurotransmitter release and synapse size. *Neuron.* 32:673–682.
5. Murthy, V. N., and C. F. Stevens. 1999. Reversal of synaptic vesicle docking at central synapses. *Nat. Neurosci.* 2:503–507.
6. Ryan, T. A., H. Reuter, and S. J. Smith. 1997. Optical detection of a quantal presynaptic membrane turnover. *Nature.* 388:478–482.
7. Ryan, T. A., and S. J. Smith. 1995. Vesicle pool mobilization during action potential firing at hippocampal synapses. *Neuron.* 14:983–989.
8. Ryan, T. A., L. Li, …, S. J. Smith. 1996. Synaptic vesicle recycling in synapsin I knock-out mice. *J. Cell Biol.* 134:1219–1227.
9. Fernández-Alfonso, T., and T. A. Ryan. 2004. The kinetics of synaptic vesicle pool depletion at CNS synaptic terminals. *Neuron.* 41:943–953.
10. Murthy, V. N., and C. F. Stevens. 1998. Synaptic vesicles retain their identity through the endocytic cycle. *Nature.* 392:497–501.
11. Smith, C. B., and W. J. Betz. 1996. Simultaneous independent measurement of endocytosis and exocytosis. *Nature.* 380:531–534.
12. Rosenmund, C., and C. F. Stevens. 1996. Definition of the readily releasable pool of vesicles at hippocampal synapses. *Neuron.* 16:1197–1207.
13. Denker, A., K. Kröhnert, and S. O. Rizzoli. 2009. Revisiting synaptic vesicle pool localization in the *Drosophila* neuromuscular junction. *J. Physiol.* 587:2919–2926.
14. Henkel, A. W., J. Lübke, and W. J. Betz. 1996. FM1-43 dye ultrastructural localization in and release from frog motor nerve terminals. *Proc. Natl. Acad. Sci. USA.* 93:1918–1923.
15. Opazo, F., A. Punge, …, S. O. Rizzoli. 2010. Limited intermixing of synaptic vesicle components upon vesicle recycling. *Traffic.* 11:800–812.
16. Betz, W. J., and G. S. Bewick. 1992. Optical analysis of synaptic vesicle recycling at the frog neuromuscular junction. *Science.* 255:200–203.
17. Ryan, T. A., H. Reuter, …, S. J. Smith. 1993. The kinetics of synaptic vesicle recycling measured at single presynaptic boutons. *Neuron.* 11:713–724.
18. Miesenböck, G., D. A. De Angelis, and J. E. Rothman. 1998. Visualizing secretion and synaptic transmission with pH-sensitive green fluorescent proteins. *Nature.* 394:192–195.
19. Sankaranarayanan, S., and T. A. Ryan. 2000. Real-time measurements of vesicle-SNARE recycling in synapses of the central nervous system. *Nat. Cell Biol.* 2:197–204.
20. Adie, E. J., S. Kalinka, …, S. Game. 2002. A pH-sensitive fluor, CypHer 5, used to monitor agonist-induced G protein-coupled receptor internalization in live cells. *Biotechniques.* 33:1152–1154, 1156–1157.
21. Martens, H., M. C. Weston, …, W. Härtig. 2008. Unique luminal localization of VGAT-C terminus allows for selective labeling of active cortical GABAergic synapses. *J. Neurosci.* 28:13125–13131.
22. Murthy, V. N., T. J. Sejnowski, and C. F. Stevens. 1997. Heterogeneous release properties of visualized individual hippocampal synapses. *Neuron.* 18:599–612.
23. Branco, T., K. Staras, …, Y. Goda. 2008. Local dendritic activity sets release probability at hippocampal synapses. *Neuron.* 59:475–485.
24. Branco, T., V. Marra, and K. Staras. 2009. Examining size-strength relationships at hippocampal synapses using an ultrastructural measurement of synaptic release probability. *J. Struct. Biol.* 172:203–210.
25. Branco, T., and K. Staras. 2009. The probability of neurotransmitter release: variability and feedback control at single synapses. *Nat. Rev. Neurosci.* 10:373–383.
26. Pierce, J. P., and L. M. Mendell. 1993. Quantitative ultrastructure of Ia boutons in the ventral horn: scaling and positional relationships. *J. Neurosci.* 13:4748–4763.
27. Sankaranarayanan, S., D. De Angelis, …, T. A. Ryan. 2000. The use of pHluorins for optical measurements of presynaptic activity. *Biophys. J.* 79:2199–2208.
28. Threadgill, R., K. Bobb, and A. Ghosh. 1997. Regulation of dendritic growth and remodeling by Rho, Rac, and Cdc42. *Neuron.* 19:625–634.
29. Groemer, T. W., and J. Klingauf. 2007. Synaptic vesicles recycling spontaneously and during activity belong to the same vesicle pool. *Nat. Neurosci.* 10:145–147.
30. Rizzoli, S. O., and W. J. Betz. 2004. The structural organization of the readily releasable pool of synaptic vesicles. *Science.* 303:2037–2039.
31. Manders, E. M. M., F. J. Verbeek, and J. A. Aten. 1993. Measurement of co-localization of objects in dual color confocal images. *J. Microsc.* 169:375–382.
32. Aravanis, A. M., J. L. Pyle, and R. W. Tsien. 2003. Single synaptic vesicles fusing transiently and successively without loss of identity. *Nature.* 423:643–647.
33. Richards, D. A., J. Bai, and E. R. Chapman. 2005. Two modes of exocytosis at hippocampal synapses revealed by rate of FM1-43 efflux from individual vesicles. *J. Cell Biol.* 168:929–939.
34. Cohen, J. 1988. Statistical Power Analysis for the Behavioral Sciences. Lawrence Erlbaum, Mahwah, NJ.
35. Minerbi, A., R. Kahana, …, N. E. Ziv. 2009. Long-term relationships between synaptic tenacity, synaptic remodeling, and network activity. *PLoS Biol.* 7:e1000136.
36. Chen, X., S. Barg, and W. Almers. 2008. Release of the styryl dyes from single synaptic vesicles in hippocampal neurons. *J. Neurosci.* 28:1894–1903.
37. Schikorski, T., and C. F. Stevens. 2001. Morphological correlates of functionally defined synaptic vesicle populations. *Nat. Neurosci.* 4:391–395.
38. Schwarz, G. 1978. Estimating the dimension of a model. *Ann. Stat.* 6:461–464.
39. Prange, O., and T. H. Murphy. 1999. Correlation of miniature synaptic activity and evoked release probability in cultures of cortical neurons. *J. Neurosci.* 19:6427–6438.
40. Sara, Y., T. Virmani, …, E. T. Kavalali. 2005. An isolated pool of vesicles recycles at rest and drives spontaneous neurotransmission. *Neuron.* 45:563–573.
41. Balaji, J., and T. A. Ryan. 2007. Single-vesicle imaging reveals that synaptic vesicle exocytosis and endocytosis are coupled by a single stochastic mode. *Proc. Natl. Acad. Sci. USA.* 104:20576–20581.
42. Pieribone, V. A., O. Shupliakov, …, P. Greengard. 1995. Distinct pools of synaptic vesicles in neurotransmitter release. *Nature.* 375:493–497.
43. Wu, L. G., and W. J. Betz. 1996. Nerve activity but not intracellular calcium determines the time course of endocytosis at the frog neuromuscular junction. *Neuron.* 17:769–779.